Chinese Chemical Letters 33 (2022) 4740–4745

Contents lists available at ScienceDirect

Chinese Chemical Letters

journal homepage: www.elsevier.com/locate/cclet

Degradation of florfenicol in a flow-through electro-Fenton system enhanced by wood-derived block carbon (WBC) cathode

Li Tian[a,b], Qiongfang Zhuo[a,c,*], Jincheng Lu[a], Jingjing Liu[a], Xiaofeng Xu[a], Xiaolin You[a,b], Manman Xu[a], Bo Yang[b], Junfeng Niu[a]

[a] School of Environment and Civil Engineering, Dongguan University of Technology, Dongguan 523808, China
[b] College of Chemistry and Environmental Engineering, Shenzhen University, Shenzhen 518060, China
[c] Guangdong Provincial Key Laboratory of Environmental Pollution Control and Remediation Technology (Sun Yat-sen University), Guangzhou 510275, China

ARTICLE INFO

Article history:
Received 26 September 2021
Revised 16 December 2021
Accepted 30 December 2021
Available online 4 January 2022

Keywords:
Wood-derived block carbon
Natural multi-channel structure
Flow-through mode
Electro-fenton
Anodic oxygen

ABSTRACT

The flow-through electro-Fenton (EF-T) reactor with WBC cathode was designed to remove florfenicol (FF). The activated WBC cathode was prepared by facile carbonization and activation methods, and featured high specific surface area, natural multi-channel structure, abundant oxygen-containing groups, good hydrophilicity, and excellent O_2 reducing capacity. WBC cathode was located above Ti/Ru-IrO_2 mesh anode. O_2 evolved at the anode was carried to the inner wall of channel of WBC by the force of buoyancy and water flow, which increases oxygen source of H_2O_2 generation at the cathode. The flow-through system by using WBC electrode promote the mass transfer of O_2 and FF. The production amount of H_2O_2 at activated WBC was 32.2 mg/L, which was almost twice as much as that at non-activated WBC (15.0 mg/L). FF removal ratio in EF-T system was 98%, which was much higher than that of traditional flow-by electro-Fenton (EF-B, 33%) or single electrooxidation system (EO, 16%). EF-T system has the lowest energy consumption (4.367 kWh/kg) among the three electrochemical systems. The cathodic adsorption, anodic electrooxidation, and EF reaction are responsible for the degradation of FF. After five consecutive cycle experiments, FF removal ratio was still 98%, indicating WBC has the good stability.

In electrochemical oxidation, the degradation mechanisms of organic pollutants are direct electrochemical oxidation *via* direct electron transfer Eq. 1 [1] and indirect electrochemical oxidation, in which $^{\bullet}OH$ with $E^{o} = 2.8$ V/SHE as the main oxidative species to remove pollutants *via* Eqs. 2 and 3 [2,3]. Hydroxyl radicals ($^{\bullet}OH$) contribute to the non-selective oxidative degradation and efficient mineralization of organic pollutants [4,5]. Aside from degradation reactions, side reactions also occur, such as oxygen evolution reaction (OER) at the anode and hydrogen evolution reaction (HER) at the cathode [6]. If O_2 and H_2 were not used, the two reactions would lead to energy consumption. For EF technology, O_2 dissolved in water can be electro-reduced into H_2O_2 and then produce $^{\bullet}OH$ in the presence of Fe^{2+} according to Eqs. 4 and 5 [7,8]. It is a feasible method to enhance the oxidation removal efficacy of pollutants by combining the oxidation process of anode and cathode [9]. Furthermore, oxygen reduction reaction (ORR) can partly replace HER at the cathode and save energy consumption. However, the traditional EF processes require external aeration to increase the available O_2 at the cathode because of the low content of dissolved O_2 in aqueous solution and the limitation of mass transfer, resulting in additional costs and energy consumption [10,11]. OER is an inevitable process, and it causes a waste of energy. O_2 produced in OER processes is exactly what ORR/EF needs. Therefore, if O_2 evolved at the anode can be totally introduced to the cathode surface to electro-reduce into H_2O_2, the degradation performance would be improved, and the utilization rate of electric energy would be increased.

$$\text{Pollutants} \rightarrow \text{Products} + e^{-} \quad (1)$$

$$M + H_2O \rightarrow M(^{\bullet}OH) + H^{+} + e^{-} \quad (2)$$

$$M(^{\bullet}OH) \rightarrow MO + H^{+} + e^{-} \quad (3)$$

$$O_2 + 2e^{-} + 2H^{+} \rightarrow H_2O_2 \quad (4)$$

$$H_2O_2 + Fe^{2+} \rightarrow Fe^{3+} + OH^{-} + {}^{\bullet}OH \quad (5)$$

* Corresponding author.
E-mail address: zhuoqf@dgut.edu.cn (Q. Zhuo).

https://doi.org/10.1016/j.cclet.2021.12.083
1001-8417/

In the EF system, the contact path and reduction behavior of O_2, which depends on the structure and properties of the cathode material, at the cathode are crucial to obtain a large amount of H_2O_2. Carbonaceous materials, especially porous carbon materials, such as carbon nanotube [12], carbon sponge [13], activated carbon fiber [14], and carbon modified with metals or metal oxides nanoparticles [15], have drawn significant concern due to the high specific surface area, large porosity, excellent chemical stability, satisfactory electrical conductivity, high selectivity of two-electron ORR, and low cost. Selection and preparation of porous carbon materials primarily depends on precursor. For instance, pyrolysis of electron-spun polyacrylonitrile for carbon nanofiber [16], chemical vapor deposition with catalyst or template sacrifice method for carbon nanotube sponge [17], and facile pyrolysis of a metal-organic framework for hollow graphene nano-spheres [18] were reported. Although the aforementioned porous carbon materials are often used as high-efficiency EF cathodes, they usually suffer from complex preparation processes and unsatisfactory mechanical strength. Natural wood is associated with human life given its reproducibility, environment friendliness, and richness. Natural wood can be employed as a precursor of carbon cathodic materials in the EF system owing to porous and fibrous structural tissue in the stems and roots of trees [19]. Compared with other porous carbon materials based on wood, such as sawdust-derived charcoal [20], wood-derived biochar powder [21], wood carbon fiber [22], and wood carbon sphere [23], WBC materials retain natural interspace channels and have the advantages of easy preparation, hierarchical porosity, self-supporting without other templates or adhesives, and extensive compatibility [24]. WBC has been reported as EF cathode, showing good performance due to its unique structure and properties, which are favorable for the permeation of O_2 and ORR [25,26].

The flow-through electrochemical system can decrease the thickness of the diffusional layer to the value, which is similar to the pore radius, increase the mass transfer and enhance the degradation ratios [27–29]. The natural interspace channels in WBC are suitable to be fabricated as the flow-through cathode in the EF system. Considering that O_2 evolved at the anode can be employed as the oxygen source for EF reactions, the flow-through reactor enhanced by the anodic O_2 were manufactured, in which the anode was located under the cathode. O_2 evolved at the anode naturally flows upward to the cathodic channels and facilitates the production of H_2O_2 at the cathode. In the presence of Fe^{2+}, the electrogenerated H_2O_2 can continuously produce $^{\bullet}OH$, enhance oxidation, and increase energy efficiency. The innovation of this study is the flow-through EF reactor with WBC cathode was fabricated, in which all O_2 evolved at the anode can reach to the cathode and be fully utilized as the oxygen source for EF reactions. This technology can replace the traditional EF method, in which aerations are usually used as the oxygen source and increase the power expenses. The synergistic effects of cathode adsorption, anodic electrooxidation, and electro-Fenton reaction would lead to high pollutant removal ability.

The preparation processes of CO_2-activated WBC included carbonization and CO_2 activation steps (Fig. 1a), which were described in detail in Supporting information (Text S1). The SEM images of WBC in the top direction present (Fig. 1b) many highly ordered channels with a diameter of 10–50 μm, confirming that high-temperature carbonization in the Ar atmosphere could make the wood retain the natural structure instead of collapse. Moreover, the SEM spectrum in the lateral direction (Fig. 1c) indicates that all the channels are aligned from top to bottom, which facilitates the rapid passage of gas or liquid through the electrode material [25]. WBC features good penetrability because the light transmission phenomena can be observed (Fig. S1 in Supporting information). A large number of irregular holes (1–1.5 μm) appear at the walls of the channels (Fig. 1d), indicating that WBC has a multi-porous structure. The excellent three-dimensional interconnected porous framework structure can prolong the residence time inside the electrode and promote the degradation reactions [30]. Compared with the non-activated WBC (Fig. 1d), the surface of CO_2-activated WBC (Fig. 1e) becomes rough and presents many nanoscale pores, which would increase the surface area and the number of active sites.

The BET analyses of non-activated and CO_2-activated WBC (Fig. 1f) reflect the existence of abundant micropore structure [30]. Two peaks appear at 0.73 and 0.80 nm for non-activated WBC (Fig. 1g). After activation, except for the two peaks, three new peaks emerge at 0.59, 0.86, and 0.93 nm for CO_2-activated WBC (Fig. 1g), indicating that the activation process can etch the pits and produce new micropores. The specific surface area of CO_2-activated WBC (1512.97 m^2/g) is higher than that of non-activated WBC (853.13 m^2/g) (Table S1), indicating that CO_2 activation can increase the specific surface area.

XPS (Fig. S2 in Supporting information) analyses show that non-activated and CO_2-activated WBC contain C and O. The peak intensity at binding energy of 533 eV attributed to the epoxy group (C−O−C) [31] of CO_2-activated WBC is higher than that of non-activated WBC (Fig. 1h), leading to more active sites for ORR [32]. The contact angle of CO_2-activated WBC is lower than that of non-activated WBC (Fig. S3 in Supporting information), which demonstrated the higher hydrophilicity after the activation process.

The Raman results (Fig. 1i) showed the characteristic peaks of two electrodes at ~1342 and ~1582 cm^{-1}, which represent amorphous carbon-induced D band and graphite carbon-induced G band, respectively [33]. The I_D/I_G ratio of CO_2-activated WBC is 0.985, which is lower than that of non-activated WBC (1.038), indicating that the activation process increased the graphitization. Therefore, CO_2-activated WBC has better electrical conductivity, which plays an important role in efficient electrochemical application [31].

The amount of H_2O_2 produced was determined using a hollow square column (HSC) reactor with flow-through mode (Fig. 2a). Additional detailed parameters can be seen in Supporting information (Text S2). When the constant current of 20 mA was applied, non-activated and CO_2-activated cathodes can produce H_2O_2. The H_2O_2 yield (32.2 mg/L) at the activated WBC is almost twice as much as that at the non-activated WBC (15.0 mg/L) Fig. 2b). The current efficiencies at activated and non-activated WBC are 33.8% and 15.8% (inset in Fig. 2b), respectively. When the potential was −1 V (*vs.* SCE), the electrochemical test showed higher current density at the CO_2-activated WBC (−11.02 mA/cm^2) than that at the non-activated WBC (−6.17 mA/cm^2). This finding confirmed that the activated cathode has stronger reduction ability and favors the accumulation of H_2O_2 (Fig. S4 in Supporting information) [31]. On the one hand, the higher specific surface area provides more reactive sites for O_2 reduction [32], and higher hydrophilicity offers more contact between O_2 and cathode surfaces. On the other hand, the larger pore volume (0.5937 cm^3/g) facilitates O_2 to diffuse inside the cathode and prolong the stagnation time [34]. In addition, the improvement of electrical conductivity effectively improves the ability of electron transfer, which is conducive to ORR. Therefore, CO_2-activated WBC was adopted as the cathode in the following experiments.

Working current is an important parameter in electrochemical oxidation systems due to its involvement in electron transfer speed and energy consumption. Therefore, the influence of current on H_2O_2 accumulation was investigated (Fig. 2c). The amounts of H_2O_2 produced are 21.9, 32.2, 34.6, and 35.7 mg/L at currents of 15, 20, 30, and 40 mA, respectively. The accumulation of H_2O_2 increases as the current increases. No significant improvement in H_2O_2 production occurred when the current was higher than 20 mA. The highest value of current efficiency is 33.8% at a current

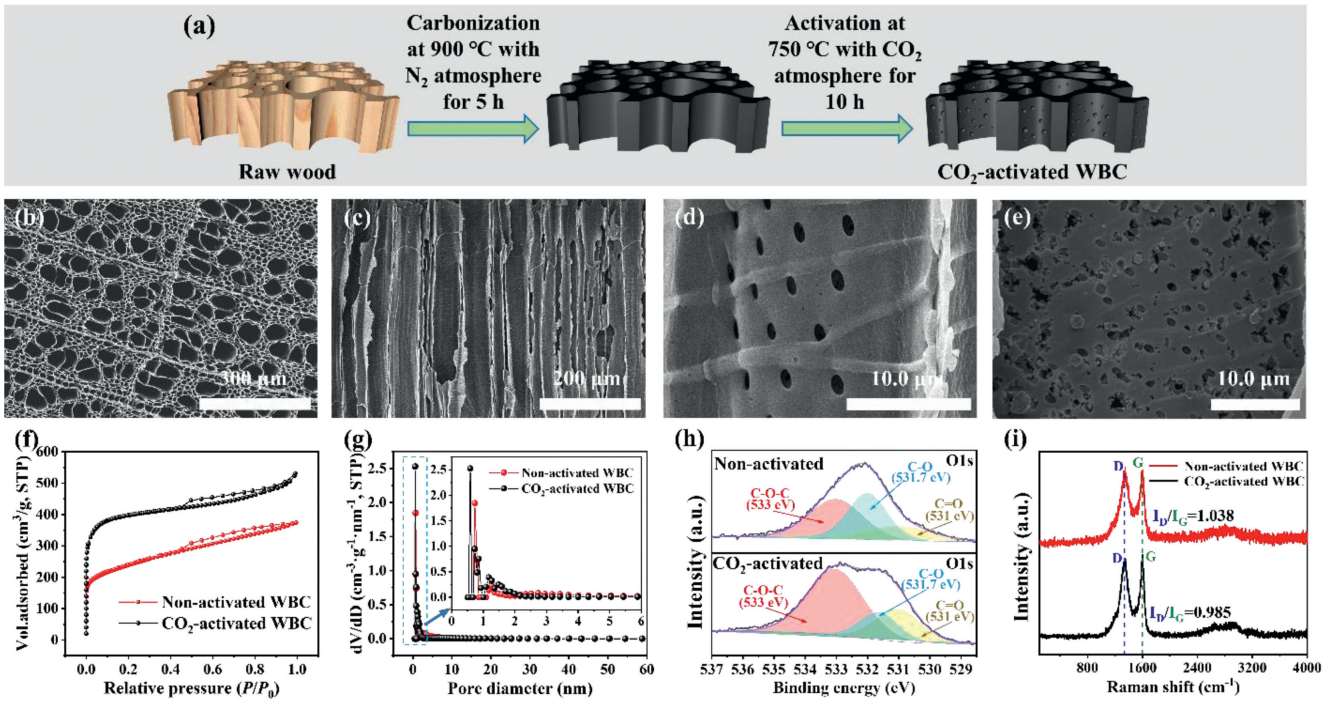

Fig. 1. (a) Fabrication processes of WBC, (b–e) SEM images, (f) N_2 adsorption isotherms, (g) pore size distribution, (h) O 1s XPS spectra, and (i) Raman spectra.

of 20 mA (inset in Fig. 2c), but it decreases sharply with increasing current (24.2% at 30 mA and 18.8% at 40 mA). The hydrogen evolution potential of CO_2-activated WBC was −1.31 V (*vs.* SCE, Fig. S5). With the increase in the current, the cathodic potentials were below −1.31 V (Table S2 in Supporting information), indicating the higher currents accelerate the rate of HER side reaction and lead to the decreasing current efficiency of H_2O_2 generation [35]. Other possible parasitic reactions occurred, including the electrochemical reduction of H_2O_2 at the cathode, the electrochemical oxidation of H_2O_2 at the anode, and H_2O_2 disproportionation in the bulk solution [25]. Although the maximum H_2O_2 content was obtained at a current of 40 mA, 20 mA was regarded as more practical due to the highest current efficiency obtained. As a consequence, 20 mA was chosen as the optimal current in the following experiments.

The effects of reactor configurations [the electrochemical oxidation with the Ti/Ru-IrO_2 anode in the flow-by mode (EO-B), the electrochemical oxidation coupled with EF in the flow-by mode (EF-B) with an aerator, and the electrochemical oxidation coupled with EF in the flow-through mode (EF-T) without an aerator] on the degradation of FF were investigated (Fig. S6 in Supporting information). Comparison experiments were carried out under the same conditions (200 mL, 50 mmol/L Na_2SO_4 electrolyte, 100 mg/L FF, pH 3, and current = 20 mA), and the experiments results are shown in Fig. 2d. In EF-B and EF-T systems, 0.25 mmol/L Fe^{2+} was added to the electrolyte. Within 90 min, the FF removal was only 16% in the EO-B system after electrolysis for 90 min, suggesting that single anodic oxidation was not efficient in flow-by mode. A boost occurred in EF-B when aeration and Fe^{2+} were added, and the FF removal reached 33%. The higher removal efficiency of FF proved that pollutant degradation was enhanced by EF derived from indirect cathodic oxidation. The FF removal efficiency was significantly improved to 98% in the EF-T system, which is higher than that in EO-B and EF-B systems. At this point, it is essential to mention that no aeration equipment was employed in the EF-T system. Such significant improvement might be attributed to the electroreduction process of O_2. In the EF-T system, the anode released a high concentration of dissolved O_2 and tiny bubbles of pure O_2 gas, which almost completely reached the internal surface of the nature channel in the WBC cathode due to the driving force of buoyancy and pump. A large number of active sites and oxygen-containing functional groups at WBC facilitated the electroreduction of O_2 into H_2O_2 [32]. By contrast, the EF-B system with the flow-by mode is limited by two factors. The first factor is that gas bubbles derived from the aerator are not pure O_2 molecules. The second factor is that the mass transfer of O_2 from the solution to the cathodic surface and inside the nature channels in WBC is insufficient with traditional magnetic agitator. Therefore, when the anodic O_2 was correctly imported into the nature channels in WBC, the degradation ratios can be greatly improved, and the pump energy can be saved. The specific energy consumptions of the three electrochemical systems were calculated (Fig. 2e). The EO-B system resulted in the highest energy consumption of 25.0 kWh per kilogram of FF. A significant decrease occurred when electro-Fenton was employed in the EF-B system (11.6 kWh per kilogram of FF). The lowest energy consumption (4.4 kWh per kilogram of FF) was found in flow-through mode. Total organic carbon (TOC) test was conducted to assess the system's ability to mineralize florfenicol (Fig. 3a). When FF was completely removed (120 min), TOC removal ratio was 74.9%. After 360 min of electrolysis, TOC removal ratio was up to 92.4%, indicating EF-T system had the high mineralization capacity. These strong lines of evidence prove that the EF-T system has promising practical application prospect because of its high capacity for decontamination and low cost. pH is an important parameter that affects the electrochemical process given that Fe^{2+} is very sensitive in various pH environments [36]. As shown in Fig. S7a (Supporting information), the preferable removal efficiencies were obtained when the range of pH was between 2 and 3. Under higher acidic conditions (pH 2), the removal efficiency is slightly lower than that at pH 3. Such results might be due to the presence of a large number of H^+ in the strong acid environment, triggering a competitive reaction (HER), which inhibits the electroreduction generation of H_2O_2 and Fe^{2+} [36,37]. When the pH value is higher than 3, the removal effects of FF gradually decreased, which might be due to the irreversible deactivation of iron ions [38]. In

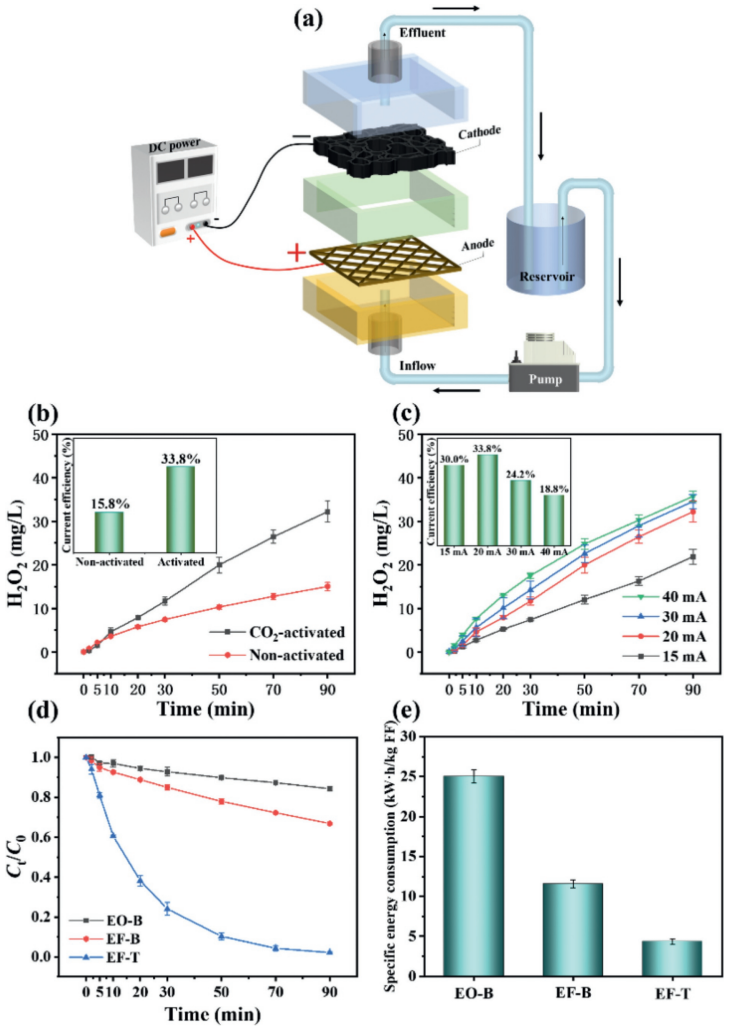

Fig. 2. (a) Schematic diagram of HSC, (b) H_2O_2 accumulation at CO_2-activated WBC and non-activated WBC, (c) effect of current on H_2O_2 accumulation using CO_2-activated WBC, (d) degradation of FF and (e) specific energy consumption of EO-B, EF-B, and EF-T systems, respectively.

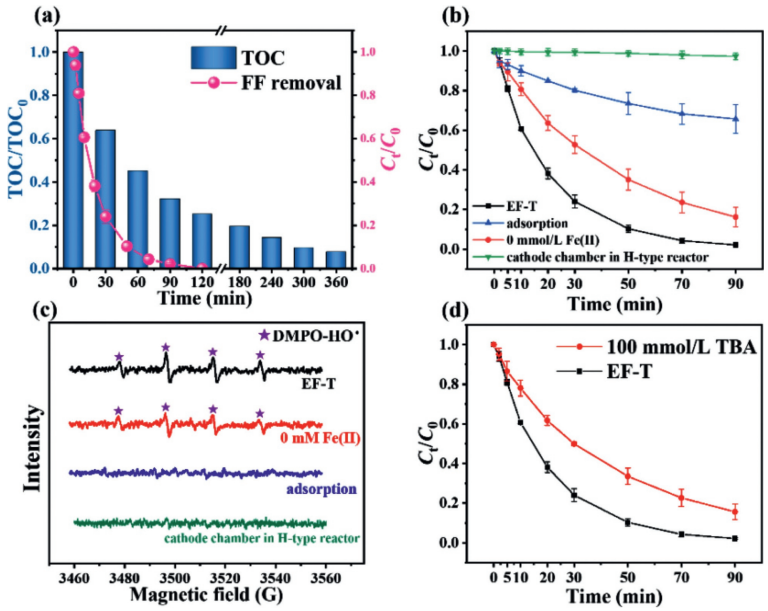

Fig. 3. (a) FF concentration and TOC variations as a function of electrolysis time. (b) FF removal and (c) electron paramagnetic resonance spectra of ·OH trapped by 100 mmol/L DMPO at different experimental conditions. (d) Effects of TBA on the FF removal.

subsequent experiments, pH value in FF solution was adjusted to 3 with H_2SO_4 before degradation. The amount of Fe^{2+} in the solution directly affected the transformation of H_2O_2, so the effect of the initial Fe^{2+} concentration was also investigated. As shown in Fig. S7c (Supporting information), the FF concentration gradually decreases with increasing initial Fe^{2+} concentration. Although the results indicated that the increase in the Fe^{2+} concentration in the system improved the efficiency of the Fenton reaction, the doubling of Fe^{2+} concentration did not result in a corresponding increase. This experimental phenomenon was ascribed to the facts that the low concentration of H_2O_2 restricted Fenton reaction and ·OH was quenched by redundant Fe^{2+} [39]. Different initial FF concentrations were also used to investigate the decontamination capacity in the EF-T system. As shown in Fig. S7e (Supporting information), the removal ratios in the initial concentration range of 50–200 mg/L were all higher than 92% within 90 min, indicating that the system has the high oxidation ability to treat high concentrations of wastewater, such as medical wastewater from pharmaceutical production plants [40,41]. The long-term work of electrochemical systems is a critical factor in practical application. The FF removal efficiency kept almost 98% after five consecutive cycle experiments (Fig. S8a in Supporting information). The apparent kinetic rate constants are within 0.0418 to 0.0478 min^{-1} (Fig. S8b in Supporting information), indicating the high stability of the system. The SEM images (Figs. S8c-e in Supporting information) of the WBC cathode after the stability test experiments present that the surface morphologies of WBC materials are nearly the same as that of the original ones, indicating that WBC has good mechanical and chemical stability. The investigation of the system stability affected by impurities such as cations/anions and organic compounds was considered. Different ions (Cl^-, NO_3^-, NH_4^+ and Ca^{2+}, each ion with the concentration of 100 mg/L) were added to the electrolyte solution to investigate the effect of each ion on FF removal. Fig. S9 (Supporting information) shows that all kinds of anions or cations had no obvious effect on the removal of FF in the electrochemical system. In addition, the effects of acetamidophenol (ACT, 100 mg/L) and carbamazepine (CBZ, 100 mg/L) on the degradation of FF were also investigated (Fig. S9). The experimental results showed that FF degradation ratios decreased in the presence of ACT or CBZ due to the competition reactions. Landfill leachate wastewater after biochemical treatment (Table S4 in Supporting information for the detailed information of its composition) was selected to evaluate the actual wastewater treatment ability of EF-T system. Fig. S10 (Supporting information) shows that COD decreased from 301.2 to 97.8 mg/L after 3 h of electrolysis at the current of 20 mA, indicating EF-T system had a high oxidation ability to treat actual wastewater. In addition, after five consecutive cycles of operation, COD removal efficiencies remained above 66%, which proved that EF-T system had good stability in the treatment of actual wastewater.

Condition experiments were performed in the HSC reactor to distinguish the contribution of the Ti/Ru-IrO_2 anode and CO_2-activated WBC cathode in FF removal. As shown in Fig. 3b, the FF removal rate of 35% was achieved under the adsorption condition without any working current. This result is attributed to the high specific surface area and well-developed pore structure of the CO_2-activated WBC cathode [42]. In electrochemical oxidation without Fe^{2+}, the FF removal ratio increased to 84%. The electro-generation of H_2O_2 occurred in the electrochemical oxidation process. In order to clarify the H_2O_2 activation mechanisms, H-type electrochemical reactor was prepared, in which the cathode and anode were separated by Nafion 117 membrane. The electrolyte of cathode chamber contained 50 mmol/L Na_2SO_4 and 100 mg/L FF at pH 3. No Fe^{2+} was added during the experiment. When a constant current of 20 mA was applied, the production amounts of H_2O_2 increased with the time increase (Fig. S11a in Supporting information), but

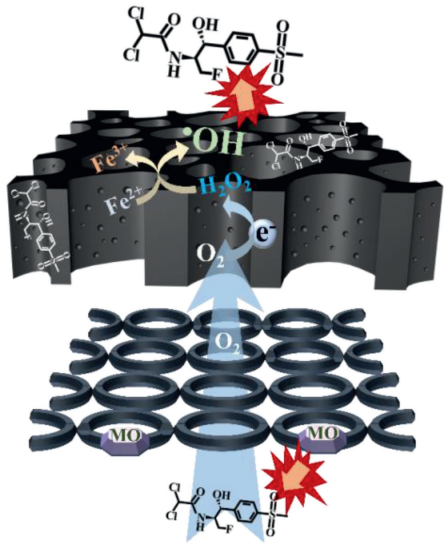

Fig. 4. The degradation mechanisms of FF in EF-T system.

there was no significant decrease in FF concentration, which indicated that H_2O_2 can neither degrade FF directly nor were activated by cathode. In addition, EPR test (Fig. S11b in Supporting information) was conducted, and no obvious characteristic peak was found, indicating that H_2O_2 could not produce ·OH at WBC cathode through direct electron transfer. Therefore, FF removal in the electrochemical oxidation system without Fe^{2+} was responsible for anodic electrooxidation and cathodic adsorption. When Fe^{2+} was employed, H_2O_2 produced at the cathode reacted with Fe^{2+} to generate ·OH, which enhanced the decontamination of FF, and the FF removal reached 98%. The above results indicated that the decomposition mechanisms of FF mainly involved cathodic adsorption, anodic oxidation, and indirect oxidation by electro-Fenton, whose contributions were 35%, 49%, and 14%, respectively [30], according to calculations of FF removals (Fig. 3b).

Electron paramagnetic resonance (EPR) analysis was carried out to identify oxidative species in the three removal processes [43]. As shown in Fig. 3c, no characteristic peaks were found in the EPR spectra in the adsorption process, confirming the occurrence of cathodic adsorption. In the electrochemical oxidation process without Fe^{2+}, the ·OH signal peaks were detected, indicating that ·OH was produced at the Ti/Ru-IrO_2 anode [2]. The intensity of ·OH signal peaks were the strongest among the three experiments when Fe^{2+} existed. These results suggested that the electro-Fenton reaction dramatically enhanced the generation of ·OH by anodic O_2. A quenching experiment was also conducted to verify the role of ·OH in the degradation process of FF (Fig. 3d). The removal ratios of FF were reduced from 98% to 84%, and the apparent kinetic rate constants decreased from 0.0436 min^{-1} to 0.0206 min^{-1} after adding 100 mmol/L TBA (Fig. S13 in Supporting information). Hence, ·OH played a crucial role in pollutant oxidation processes [44].

Based on the above results, the degradation mechanisms of FF in the electro-Fenton system assisted by O_2 evolved at the anode are shown in Fig. 4. The Ti/Ru-IrO_2 anode produces hydroxyl radicals and partly forms oxidized active substances (MO), which can oxidize FF. At the same time, O_2 generated at the anode diffuses into the CO_2-activated WBC cathode with the help of water flow and buoyancy. Due to the hierarchical porous structure and surface oxygen-containing functional groups, O_2 can be efficiently electro-reduced to H_2O_2. In the presence of Fe^{2+}, H_2O_2 combines with Fe^{2+} to generate a large number of ·OH. In addition, cathodic adsorption plays a role in the adsorption of FF because of the high specific surface area of the cathode. Therefore, the degradation

mechanisms of FF in the EF-T system are the synergy of adsorption, MO, and •OH.

In this study, a wood-derived carbon cathode with the advantages of high specific surface area, hierarchical porous structure, abundant oxygen-containing groups, good hydrophilicity, and excellent O_2 reducing capacity was prepared by facile carbonization and activation. The flow-through electrochemical reactor with the multi-channel WBC was constructed, which pushed all O_2 produced at the anode to diffuse into the natural channel of WBC and enhanced the utilization efficiency of O_2. The results showed that the CO_2-activated WBC cathode produced more H_2O_2 by electroreducing O_2 derived from the anode. In the presence of Fe^{2+}, H_2O_2 was transformed into •OH, which enhanced the oxidation of FF. The removal efficiency of FF was as high as 98% under the optimum conditions (current of 20 mA, pH 3, 100 mg/L FF, 0.25 mmol/L Fe^{2+}, and 50 mmol/L Na_2SO_4) within 90 min. The cathodic adsorption, anodic electrooxidation, and Fenton reaction are responsible for the degradation of FF. Compared with the conventional electrochemical system, the EF-T system achieved the highest FF removal and the lowest energy consumption. In addition, the long-term working tests demonstrated that WBC had the advantage of good stability. Hence, the electro-Fenton process enhanced by anodic O_2 has potential application in advanced water purification.

Declaration of competing interest

The authors declare that they have no known competing financial interests or personal relationships that could have appeared to influence the work reported in this paper.

Acknowledgments

This work was supported by the National Science Fund for Distinguished Young Scholars (No. 51625801), Major Science and Technology Program for Water Pollution Control and Treatment in China (No. 2017ZX07202-001-007), Guangdong Province Universities and Colleges Pearl River Scholar Funded Scheme (2017), Guangdong Provincial Science and Technology Project (No. 2017A020216014), the National Natural Science Foundation of China (No. 21777106), and Pearl River S&T Nova Program of Guangzhou, China (No. 201710010065) and Guangdong Provincial Key Laboratory of Environmental Pollution Control and Remediation Technology (No. 2020B1212060022).

Supplementary materials

Supplementary material associated with this article can be found, in the online version, at doi:10.1016/j.cclet.2021.12.083.

References

[1] A. Özcan, Y. Şahin, A.S. Koparal, et al., Water Res. 42 (2008) 2889–2898.
[2] H. Guo, Z. Xu, D. Wang, et al., Chemosphere 286 (2022) 131580.
[3] O. Scialdone, S. Randazzo, A. Galia, et al., Electrochim. Acta 54 (2009) 1210–1217.
[4] C. Barrera-Díaz, P. Cañizares, F. Fernandez, et al., J. Mex. Chem. Soc. 58 (2014) 256–275.
[5] J. Wang, S. Wang, Chem. Eng. J. 401 (2020) 126158.
[6] S. Garcia-Segura, J.D. Ocon, M.N. Chong, Process Saf. Environ. Prot. 113 (2018) 48–67.
[7] Z. Wei, H. Xu, Z. Lei, et al., Chin. Chem. Lett. 33 (2022) 920–925.
[8] A. Babuponnusami, K. Muthukumar, Chem. Eng. J. 183 (2012) 1–9.
[9] M.A. Oturan, Curr. Opin. Solid State Mater. Sci. (2021) 100925.
[10] Z. Wang, M. Liu, F. Xiao, et al., Chin. Chem. Lett. 33 (2022) 653–662.
[11] X. Wang, P. Cao, K. Zhao, et al., Sep. Purif. Technol. 276 (2021) 119266.
[12] Y. Liu, F. Liu, N. Ding, et al., Chin. Chem. Lett. 31 (2020) 2539–2548.
[13] A. Özcan, Y. Şahin, A. Savaş Koparal, et al., J. Electroanal. Chem. 616 (2008) 71–78.
[14] F. Yu, Y. Wang, H. Ma, J. Electroanal. Chem. 838 (2019) 57–65.
[15] E. Brillas, I. Sirés, M. Oturan, Chem. Rev. 109 (2009) 6570–6631.
[16] B.I. Waisi, J.T. Arena, N.E. Benes, et al., Microporous Mesoporous Mater. 296 (2020) 109966.
[17] D. Kukkar, A. Rani, V. Kumar, et al., J. Colloid Interface Sci. 570 (2020) 411–422.
[18] H. Xu, X. Yin, M. Zhu, et al., Carbon 142 (2019) 346–353.
[19] H. Zhu, W. Luo, P.N. Ciesielski, et al., Chem. Rev. 116 (2016) 12650.
[20] T.E. Oladimeji, B.O. Odunoye, F.B. Elehinafe, et al., Heliyon 7 (2021) e05960.
[21] T. Wang, D. Zhang, K. Fang, et al., J. Environ. Chem. Eng. 9 (2021) 105184.
[22] Q. Huang, J. Hu, M. Zhang, et al., Chin. Chem. Lett. 33 (2022) 1091–1094.
[23] X. Zhao, W. Li, S. Zhang, et al., Mater. Chem. Phys. 155 (2015) 52–58.
[24] M. Liu, M. Xu, Y. Xue, et al., ACS Appl. Mater. Interfaces 10 (2018) 31260–31270.
[25] F. Deng, H. Olvera-Vargas, O. Garcia-Rodriguez, et al., J. Hazard. Mater. 377 (2019) 249–258.
[26] Y. Guo, S. Wu, H. Yu, et al., Water Sci. Technol. 80 (2019) 970–978.
[27] B.P. Chaplin, Acc. Chem. Res. 52 (2019) 596–604.
[28] D. Guo, Y. Liu, H. Ji, et al., Environ. Sci. Technol. 55 (2021) 4045–4053.
[29] F. Liu, Y. Liu, Q. Yao, et al., Environ. Sci. Technol. 54 (2020) 5913–5921.
[30] C. Wang, Y. Gu, S. Wu, et al., Environ. Sci. Technol. 54 (2020) 1920–1928.
[31] H.M.A. Sharif, T. Li, N. Mahmood, et al., Carbon 182 (2021) 516–524.
[32] Z. Lu, G. Chen, S. Siahrostami, et al., Nat. Catal. 1 (2018) 156–162.
[33] F. Wang, J.Y. Cheong, J. Lee, et al., Adv. Funct. Mater. 31 (2021) 2101077.
[34] Y. Liu, G. Gao, C.D. Vecitis, Acc. Chem. Res. 53 (2020) 2892–2902.
[35] M.B.C. Contreras, F. Fourcade, A. Assadi, et al., Chemosphere 237 (2019) 124447.
[36] S.O. Ganiyu, M. Zhou, C.A. Martínez-Huitle, Appl. Catal. B 235 (2018) 103–129.
[37] Y. Pang, H. Xie, Y. Sun, et al., J. Mater. Chem. A 8 (2020) 24996–25016.
[38] P. Bautista, A.F. Mohedano, J.A. Casas, et al., J. Chem. Technol. Biotechnol. 83 (2008) 1323–1338.
[39] L. Ma, M. Zhou, G. Ren, et al., Electrochim. Acta 200 (2016) 222–230.
[40] Ö. Gökkuş, Y.Ş. Yıldız, Desalin. Water Treat. 57 (2016) 24934–24945.
[41] E. Emmanuel, Y. Perrodin, G. Keck, et al., J. Hazard. Mater. 117 (2005) 1–11.
[42] L. Chen, T. Ji, L. Brisbin, et al., ACS Appl. Mater. Interfaces 7 (2015) 12230–12237.
[43] C. Guo, D. Yue, S. Wang, et al., Chin. Chem. Lett. 31 (2020) 1978–1981.
[44] Z. Yan, Z. Dai, W. Zheng, et al., Water Res. 205 (2021) 117678.